Hierarchical Control of Headroom Reserve in Solar Power Plants For Frequency Response Capability

Simon A. Julien, *Student Member, IEEE,* Amirhossein Sajadi, *Senior Member, IEEE*, Bri-Mathias Hodge *Senior Member, IEEE*

***Abstract*—Curtailment control of inverter-based variable generation sources –such as wind and solar– is showing massive economic and operational advantages for future ancillary service utility providers. In this paper, we present a highly precise curtailment control algorithm that uses a statistically optimized hierarchy of controllers to perform effective curtailment of power electronic inverters. Through a case study of one-second resolution solar irradiance data, we have compared the results of our hierarchical curtailment controller design to that of a newly operational grouping control algorithm. These results show that our hierarchical control algorithm is the more functional and reliable method for a utility meeting load demands and ancillary RegD signals with solar photovoltaics. Additionally, hierarchical control has suitable application to curtailed wind power plants, and presents the possibility of "smart-grid" control at a broader, systematic level.**

***Index Terms*—IEEE, IEEEtran, journal, LaTeX, paper, template.**

I. Introduction

NATIONAL power grids are vast and multifaceted interconnections of an abundance of technology, but traditional generation systems (such as coal, natural gas, nuclear, and hydro power) and power grid operations have remained stagnant compared to the innovation of other technological industries. However, in recent years the call for renewable and net-zero energy emissions has caused a massive shift towards modernizing national power grids with new power electronic generation devices (e.g. solar photovoltaics, wind turbines, and battery storage) [1].

Already, some smaller-scale national power systems with overwhelming amounts of renewable resources are approaching zero-emission power grids. For example, Iceland has essentially hit zero emissions using a combination of geothermal and hydro power generation. Norway (97%), Costa Rica (93%), and Canada (62%) are also quickly approaching this 100% renewable and/or zero emission goal [2]. Larger power systems without an overwhelming amount of geothermal or hydro power resources are beginning to integrate increasing amounts wind and solar photovoltaics. According to the EIA's most recent 2019 annual report, about 10% of the US's energy comes from wind and solar photovoltaics, and they have forecasted that over 30% of generation will be wind and solar by 2050 [3]. Similarly, the National Renewable Energy Laboratory (NREL) claims that the aggregation of wind, solar, hydro power, nuclear, and geothermal energies may have the 2050 US power grid operating over 80% net-zero emission generators [4].

Wind and solar are considered variable renewable energy (VRE) sources because of the intermittent and unreliable nature of wind speed and solar irradiance. As VRE becomes the dominant generation source to reduce grid emissions, these national power systems will require "smart-grid" technologies to control and mitigate instabilities that are inherited from these technologies. Without smart-grid technology, wind and solar are only allowed to participate in *day-ahead energy markets*, yet the most reliable and easily controlled generation technologies (currently natural gas and coal thermal plants) are tasked to compensate for unpredictable losses and spikes in solar or wind generation through *real-time ancillary markets*. Recent orders from the US Federal Energy Regulatory Commission (such as order 1000 [5] and 841 [6]) have opened the door for utility-scale wind, solar, and storage to provide ancillary services, so the next step is to develop the necessary smart software and control algorithms to give VRE technologies the functionality required to bid into real-time markets.

Some recent research publications have began setting the stage for this technology to become a reality. Mathematical derivations and analysis into how smart-grid, renewable technology can systematically provide ancillary support in fast frequency response and over-voltage support are laid out in [7], [8]. Other works such as [9] assume the mathematical and software abilities to control power electronic generation are complete, and focus on the hardware blueprint of building an inverter-interfaced controller. You can find related research with applications to wind power plants in [10]–[15].

Control algorithms developed in [16]–[19] tackle the pin-

S. A. Julien and B. M. Hodge are with the Electrical Computer and Energy Engineering Department at the University of Colorado Boulder, 425 UCB, Boulder, CO 80309, USA, and the Power Systems Engineering Center at the National Renewable Energy Laboratory, 15013 Denver W Pkwy, Golden, CO 80401, USA, email: {Simon.Julien,BriMathias.Hodge}@colorado.edu, {Simon.Julien,Bri.Mathias.Hodge}@nrel.gov

A. Sajadi is with the Renewable and Sustainable Energy Institute at the University of Colorado Boulder, 4001 Discovery Drive, Boulder, CO 80303, USA, email: Amir.Sajadi@colorado.edu

nacle question of: How will a utility-scale solar plant decide what precise control levels to operate each of its internal components to satisfy a requested power level without being thrown off by changing cloud coverage? Hybrid control systems [19] that contain solar, diesel generators, and/or battery storage are commonly practiced solutions today, but they still require carbon emissions and fuel costs from the operators. The method developed in [18] is an internal forecasting method that would allow a solar power plant to forecast cloud coverage and adjust accordingly. This approach is intriguing, but comes with the inherent error of probabilistic forecasting and does not provide any direct algorithm that could be easily constructed into an operational software. The real-time, grouping control method developed in [16], [17] provides a control algorithm that can react to changes in cloud coverage at second and minute time resolutions. This is the algorithm that has recently been integrated onto a 141MW Chilean power plant, which is the first entirely solar power plant that is able to bid entirely into ancillary markets.

In this paper, we have developed a hierarchical control system and algorithm for utility-scale solar photovoltaic power plant, and compared this algorithm to the grouping control method recently implemented in Chile [16]. By using a hierarchy of control layers, our algorithm has the ability to simultaneously give specified control signals to each individual inverter as well as analyze and make decisions for the entire system of inverters. In combination with a statistically optimized controller layout, this allows portions of a utility-scale solar array to dynamically overcompensate for any parts of the array that are effected by temporal cloud movements, which effectively allows the power plant to accurately and reliably satisfy an ancillary service control signal. To highlight the effectiveness of this hierarchical approach, we show case-study simulations using solar irradiance data from Oahu, Hawaii to compare the controllablity of hierarchical control vs. grouping control [16]. The hierarchical nature of our proposed algorithm allows for higher control precision, faster frequency response and ancillary support, and can be easily expanded to have multiple power plants across a power grid autonomously working together for system-wide stability. Integrating this smart-grid technology into utility scale wind, solar, and storage operations is necessary for developing a reliable power grid that operates entirely on renewable and zero-emission generation sources and will coincidentally drop the price of electricity dramatically [20] [21].

The contribution of this work is to develop a modular control system for VRE, which has yet to be matured or implemented at a large scale. By advancing the state of the art mathematical software and algorithms for efficient control of networked and modular control of solar power plants, we are advancing the capabilities of smart-grid technology to a stage closer to design and implementation.

The rest of this paper will proceed as follows: We begin by introducing the fundamentals behind control of solar photovoltaic power plants by defining key terms such as curtailment control, headroom, and maximum power point. Next, the mathematical formulation behind the algorithm of grouping control is laid out, and we point out the key “averaging" error that our hierarchical algorithm is designed to eliminate. This leads to a thorough explanation of the hierarchical control algorithm including a general description of the layers of hierarchy, mathematical formulation of the algorithms being processed within each hierarchical layer, and some useful visuals of the final product. Finally, we show simulation results of applying and simulating our hierarchical design to a case study from 1-second resolution irradiance data from Oahu, Hawaii. This allows our results to spell out exactly how effective the proposed hierarchical method of control is in relation to the existing grouping control.

II. Fundamentals of Curtailment Control and Existing Technology

Curtailment control [22] will allow utility operators to maintain a constant power output, meet load forecast with precision, perform real-time ancillary adjustments and support, or any combination of these while remaining mostly unaffected by changing weather conditions or cloud coverage. This section presents the fundamentals of solar curtailment control and reviews the existing technology that has been developed by The National Renewable Energy Laboratory (NREL) for real-time curtailment control method [16]. This technology relies on grouping solar inverters by similar power potentials (similar solar availability) and making signaling operational efficiencies to each group as a whole as illustrated in **??**.

A. Curtailing from Maximum Power Point

Curtailing a generation plant means reducing its power output to a specified fraction of its maximum power potential (MPP). Figure 1 outlines how the ratio of current (I) and voltage (V) can be adjusted to control the inverter output efficiency of a solar array. By initializing the operational efficiency of the inverter to a fractional value of it’s maximum potential, we have now given enough *headroom* to ramp the inverter efficiency up and down in order to counter-act any solar resource fluctuations and variability at the power plant. This will allow a PV plant to perform a combination of maintaining a flat power output (regardless of changing cloud cover) and instantaneously ramp generation power to meet ancillary service signals. Adjusting generation headroom is performed by increasing the voltage across the circuit. By increasing this voltage, the ratio between current and voltage falls to a sub-optimal level and the inverter power output is curtailed from the MPP for the desired headroom [24].

MPP acts as a necessary starting point for curtailment control methods to determine how much power needs to be curtailed [25]. Once the desired power reduction is set, the algorithm can then compute the efficiency at which it will correspondingly run its inverter components.

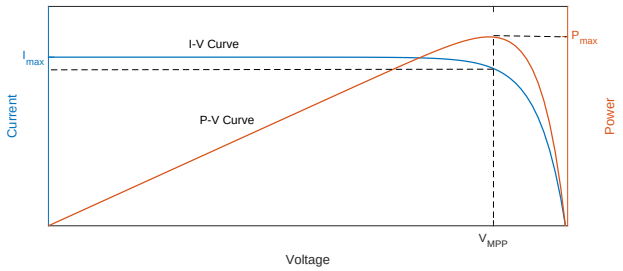

Fig. 1: IV Power curve showing relationships between voltage, current, and MPP for an individual inverter. Taken from [23].

B. Formulation of Grouping Control

The existing technology for solar curtailment is grouping method developed at NREL [16] and its principle of operation is to choose *reference inverters* to constantly operate at MPP, without curtailment, to have real-time understanding of MPP values. All other inverters, called *non-reference inverters*, are grouped with a reference inverter that has similar solar availability. This subsection reviews this technology as an algorithm and formalism.

Once reference inverters and their corresponding non-reference inverter groups have been established for the instant, [16]'s method computes the following series of calculations to determine the desired final output of each curtailed (non-reference) inverter.

The *estimated* power output capacity (P^{est}_{max}) for each group (i) is calculated by multiplying the number of inverters associated in the group ($N_{inv,i}$) with the MPP value ($P_{mpp,i}$) from the reference inverter.

$$P^{est}_{max} = \sum_{i=1}^{N_{groups}} N_{inv,i} \cdot P_{mpp,i} \tag{1}$$

Using this estimated power capacity (in Watts), the algorithm then calculates the power ($P_{set,i}$) to reduce each group to (in Watts) after curtailment (ΔP).

$$P_{set,i} = (1 - \Delta P) \cdot P^{est}_{max,i} \tag{2}$$

Finally, the power for every curtailable inverter (non-reference inverter) in each group ($P_{inv,i}$) is found by reducing curtailable inverters beyond the desired headroom level to compensate for the reference inverter always operating at MPP.

$$P_{inv,i} = \frac{P_{set,i} - P_{mpp,i}}{N_{inv} - 1} \tag{3}$$

A simple sanity check can be done by plugging in our resulting curtailment from Equation 3 into Equation 4 for the curtailed power output of the group ($P_{group,i}$).

$$\begin{aligned} P_{group,i} =& P_{mpp,i} + (N_{inv} - 1) \cdot P_{inv,i} \\ =& P_{mpp,i} + P_{set,i} - P_{mpp,i} \\ =& P_{set,i} \end{aligned} \tag{4}$$

For more detail on this similarity grouping control method, reference [16].

To evaluate the performance of this technology, we implemented the algorithm described in [16] and simulated a full day with the 17 irradinace field measurements across a site in Hawaii, (the site is described in detail in Section IV) under the simple case of maintaining a constant 20% headroom (operating at 80%) in Figure 2.

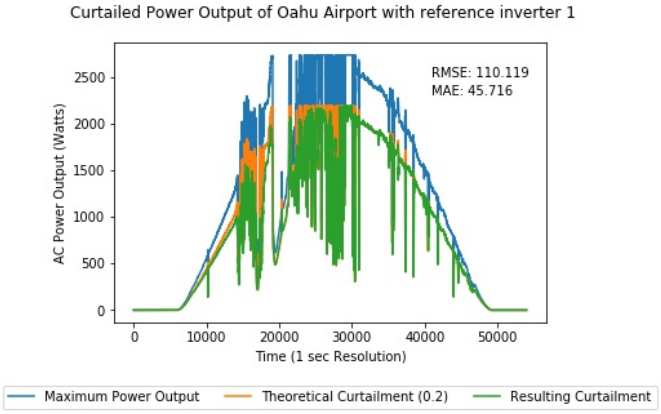

Fig. 2: Simulation results of maintaining 20% headroom for 1 partially cloudy day with grouping method.

In Figure 2, we immediately notice that there is a substantial amount of error between the theoretical curtailment performance, and the actual curtailment of our Oahu solar array. Such error could lead to inaccurate operations or problematic violations of physical constraints that exist in the hardware of the system. The paper [16] does explain that grouping the solar array with higher resolution (adding more reference inverters operating at MPP and thus reducing the range of curtailment) will reduce the error in this algorithm enough to be operational. Nonetheless, the existence of this computational error leaves room for improvement as seen in our results of Figure 9.

The source of the error in the grouping control method [16] comes from the fact that a solar panel cannot produce more power than its solar availability will allow. By using their grouping technique, all inverters of a group are assumed to have the exact amount of generation potential as their reference inverter, thus causing averaging errors. Our proposed hierarchical control solves this issue through dynamic interdependence amongst inverters.

III. Proposed Hierarchical Control Algorithm

A hierarchical control structure allows a system to be coordinated by more than one decision-making center. Necessary information is available to each controller at different time frames and at different rates. In the proposed case of implementing hierarchical curtailment control for solar photovoltaic power plants, multiple layers of decision making will ultimately allow *un-shaded* inverters to communicate and help other *shaded* inverters that cannot produce the desired curtailment value as exemplified in Figure 3b.

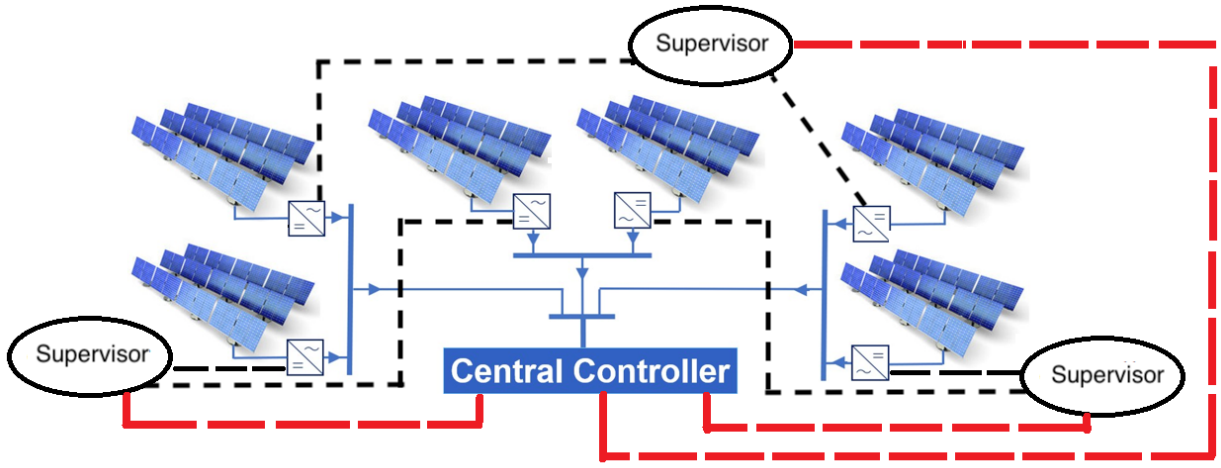

(a) Hardware layout of a hierarchical controller of power electronic inverters.

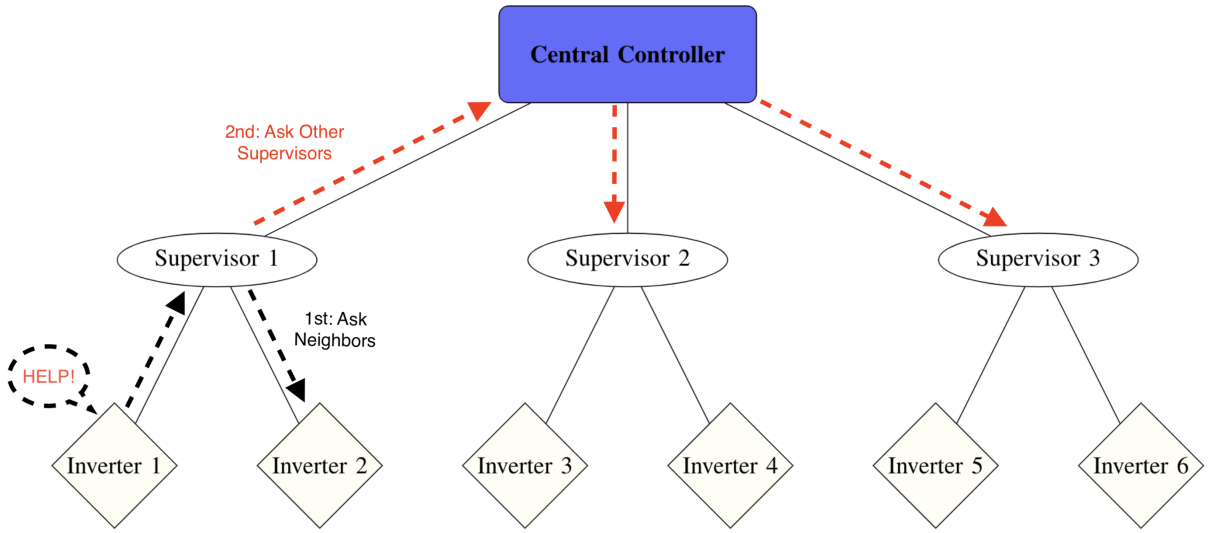

(b) "Unravelled" software layout with a signal process for the recursive algorithm of hierarchical control.

Fig. 3: Hierarchical control example with 6 inverter controllers, 3 supervisor controllers, and one central controller.

Figure 3a is a basic schematic of how the controller hardware would be implemented on a system of 6 inverters. Section 3.5 (Statistical Topology) further discusses why the structure of control signals (in red and black) follow independent paths from the power flow (in blue). Figure 3b focuses on the progression of logical decisions that the computation of the algorithm will follow to solve for a more accurate headroom request for each inverter.

The 3-layer hierarchical controller consists of an *adaptive layer* (central controller), *supervisor layer* (supervisor controllers), and a *direct control layer* (inverter controllers). Although, only three layers of control are used in this paper, one large benefit of hierarchical control is the mathematical simplicity in adding more supervisor layers (e.g. a super-supervisor layer) in order to effectively expand smart-grid control to a micro or macro sized virtual power system.

The Direct Control Layer: This hierarchical control setup extends all the way down to the the inverter level for each photovoltaic array. The *direct control layer* is the least central set of controllers, and is responsible for directly curtailing the voltage and the power output of each solar inverter. This layer initially computes the estimated maximum power potential (MPP) of an inverter and then determines if this MPP is above the requested power output. If the inverter cannot produce the requested power output, it will ask for "help" from its supervisor controller as seen in Figure 3b.

The Supervisor Layer: The supervisor control layer works as the "middle-man" of control. Supervisors first survey the performance their "children" (corresponding direct controllers). If any one of the children controllers has been flagged for needing "help", then the supervisor attempts to solve the missing amount of power generation by finding another child or children to overcompensate thier power production. If all the supervisor's children are operating at MPP and the branch is still underproducing power, the supervisor signals to the above layer

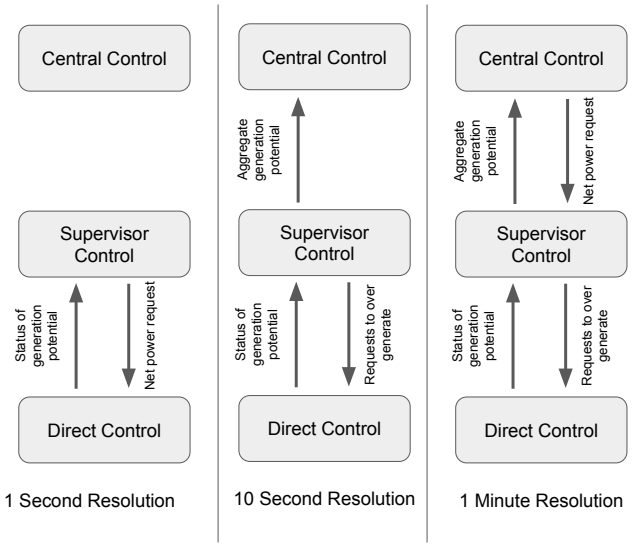

Fig. 4: General responsibilities for each hierarchical layer of control.

(adaptive central controller) that it needs support from other supervisor branches. Once the entire system has found a working solution, the supervisor signals the final curtailment requests down to each of its children.

The Adaptive Layer: The adaptive layer is at the top of the control hierarchy. It consists of one centralized controller that is only used to find solutions to underproducing supervisor control branches. If a supervisor branch is unable to produce enough power to satisfy the final demand, the adaptive layer finds alternative supervisor controllers that are reporting plenty of extra power potential within their branches. If system-wide MPP estimations are accurate, all underproduction should be resolved after reaching the adaptive layer. Final curtailment requests then flow back down from the adaptive layer, to the supervisor layer, to the direct controllers respectively as seen in Figure 4.

The following sections serve as a formulaic explanation of the chronological decision making followed by the hierarchical curtailment control algorithm. The computation is iterative and has been simulated to loop through this process once every second, however it is likely that any computational hardware could handle even higher iteration frequencies.

A. Step 1: Estimate System MPP

For any curtailment control algorithm, the maximum power penitential (MPP) must either be measured or approximated to determine a reference value for curtailment. In this method, we re-compute the MPP of each inverter after the previous iteration and use this value as the MPP estimate for the current iteration. The algorithm is continuously iterating at computational speeds much faster than solar availability is changing, so there is very little variation in MPP between iterations, which greatly reduces the error in MPP tracking from grouping control [16]. MPP tracking computations are handeled at the direct control layer.

Formulation: To re-evaluate the MPP of an inverter (i) after the previous iteration ($P^{t-1}_{mpp,i}$), the algorithm must take in the desired fractional curtailment level (α^{t-1}_i) and final (after curtailment) inverter power output ($P^{t-1}_{final,i}$) of the previous iteration ($t-1$) as arguments. Thus the formula to estimate current MPP ($P^t_{mpp,i}$) at iteration t is

$$\begin{aligned} P^t_{mpp,i} &= P^{t-1}_{mpp,i} \\ &= \frac{P^{t-1}_{final,i}}{\alpha^{t-1}_i}. \end{aligned} \tag{5}$$

The total system MPP is found by simply summing across all N inverters.

$$P^t_{mpp,system} = \sum_{i=1}^{N} P^t_{mpp,i} \tag{6}$$

B. Step 2: Compute Headroom for Controllers

Headroom is the difference between MPP and the operational level of a solar inverter after curtailment. After MPP is estimated, a uniform operational power output is requested of all inverters. Then, the difference between MPP and requested operational power (ie headroom) is computed and assigned to each inverter and each supervisor controller. This headroom value can be negative or positive, which allows it to be used as a metric of "need for assistance."

Formulation: The initial uniform power request to all inverters ($P_{request}$) is computed using the arguments of desired system power output ($P_{desired}$) and the number of inverters (N).

$$P_{request} = \frac{P_{desired}}{N} \tag{7}$$

The available headroom (H_i) at an inverter (i) is the difference between the inverter MPP value ($P_{mpp,i}$) from equation 5 and the initial power request ($P_{request}$).

$$H_i = P_{mpp,i} - P_{request} \tag{8}$$

Need of assistance for each inverter is binary:

$$H_i \geq 0 \rightarrow \text{No need of assistance}$$
$$H_i < 0 \rightarrow \text{In need of assistance}$$

The headroom value of each supervisor (H_{sup}) is found similarly by summing across $N_{children}$ "child" inverters.

$$H_{sup} = \sum_{i=1}^{N_{children}} (P_{mpp,i} - P_{request}) \tag{9}$$

Need of assistance for each supervisor is binary:

$$\sum_{i=1}^{N_{children}} H_i \geq 0 \rightarrow \text{No need of assistance}$$
$$\sum_{i=1}^{N_{children}} H_i < 0 \rightarrow \text{In need of assistance}$$

C. Step 3: Solve & Reassign Curtailment Levels

By this stage, every controller should have a stored value as their available headroom to indicate their need for operational support. Starting at the supervisor level, any controller(s) that needs help then notify the central controller exactly how much support they need. Other supervisor controllers with positive headroom values then increase their power production assignment to compensate for the negative magnitude of the struggling supervisor's headroom.

Once the power operation of each supervisor has been assigned, the process is recursively called to assign individual power curtailment operation levels for every inverter under each supervisor. Once this is complete, the algorithm can settle on a final curtailment efficiency for each inverter that will accurately achieve the desired power plant output. The hardware of the system will adjust inverter voltages accordingly.

Formulation: The amount of power (P_{help}) that needs to be overproduced is the cumulative sum of all headroom magnitudes such that $H_i < 0$. As seen in Figure 3, the algorithm then adjusts the desired production level of each controller as long as it does not exceed MPP. Figure 4 is the control logic used recursively at each level of control throughout the hierarchical control algorithm to update the operational level of the controller.

This process is followed throughout all levels of control until equilibrium is met. Equilibrium is met when $H_i \geq 0$ for all i controllers. In the final state of this system, it should be true that the desired system power output (based on the estimated MPP) is exactly equal to the sum of the final operation of each individual inverters ($P_{final,i}$).

The final step of the iteration is to solve for the curtailment fractional efficiencies (α_i) of each inverter i.

$$\alpha_i = \frac{P_{final,i}}{P_{mpp,i}} \tag{10}$$

This is used for the hardware to adjust voltage ratios, and to begin the next iteration with equation 5.

$$P = \begin{cases} P_m & \epsilon \geq 0 \\ P^* & \epsilon < 0 \end{cases} \tag{11}$$

D. Step 4: Repeat

Continuously repeat Steps 1-3 for the next iteration.

E. Step 0: Statistical Topology Optimization

An interesting aspect of the following case study in Section 4, is the use of irradiance data to theoretically optimize the power plant before building out the entire system. Although the hierarchical control technique applies fantastically to already installed solar power plants, the use of high resolution solar irradiance data for expansion modelling may be a useful technique for future power providers. This section outlines how the virtual signalling network structure of our hierarchical control model as seen in Figure 3 can be topologically optimized with sample data.

The arrangement of all the controllers within a hierarchical algorithms will greatly affect how "high up the chain" inverters will have to ask for help. For example, geographically neighboring inverters will likely have very similar solar fluctuation patterns because a passing cloud may cover both of them simultaneously. A strong hierarchical controller will chose virtual neighboring of controllers that have uncorrelated –or (ideally) inversely correlated– solar fluctuations. The term *virtual neighboring* is used to suggest that the controllers are neighbors through the eyes of the signalling hierarchy of the controller, but they not physically neighboring as visualized in Figure 6. This will make the borrowing process from Figure 3b much quicker and less computationally expensive as most controllers will find an equilibrium solution without needing to ask the centralized controller on the adaptive layer.

In the following case study, we found that the best metric to determine statistical correlation between all inverters was to perform a basic statistical learning technique that operates on a single year training set of 1 second irradiance data. Using the training set, we were able to establish a personalized n by n correlation matrix for the set of n inverters in the area. Each inverter will have a per-unit rating of their level of behavioral correlation to all the other inverters at the plant. Each correlation coefficient C is calculated by Pearson's Linear Correlation Coefficient where two time-series vectors X and Y are inputted to the function:

$$C(X,Y) = \frac{\sum_{i=1}^{t}(X_i - \overline{X})(Y_i - \overline{Y})}{\sqrt{\sum_{i=1}^{t}(X_i - \overline{X})^2 \sum_{i=1}^{t}(Y_i - \overline{Y})^2}} \tag{12}$$

This value of correlation (C) between two inverters, inv and n, is placed into the n by n correlation matrix as seen in Figure 5. Using the final statistical characterization of the solar variation between power plant inverters through from correlation matrix, hierarchical tiers with non-similar or inversely correlated fluctuation patterns can be chosen as virtual neighbors for optimal power output stability.

IV. Case Study Oahu, Hawaiian Airport

The control method developed in this project may apply to any geographic setting with potential for lucrative solar arrays. However, our simulation results were created by applying our control algorithm to a SIMULINK controller design that is simulated at the Oahu, Hawaii airport. The data that we have available for this study has 1-second resolution irradiance measurements from 17 devices around the airport. These irradiance meters measured starting at 5am and ending at 8pm, every day, April through October, in both 2010 and 2011. In Figure 6, the layout of the measured data is presented visually through a satellite image with solar PV graphics marking the location of each irradiance meter.

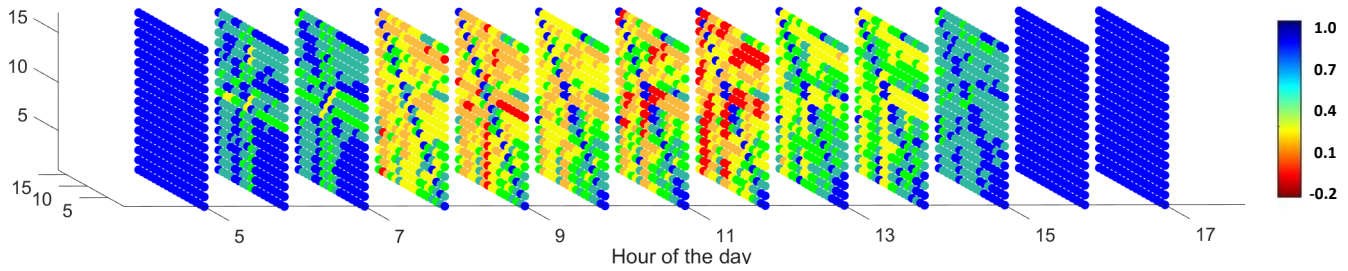

Fig. 5: Correlation heat map for all 17 inverters for every hour of operation throughout the day. Blue signifies high direct correlation, and red suggests inverse correlation. The blue diagonal is expected because each inverter should have a correlation of 1 with itself.

A. Solar Irradiance Data to AC Power Formulation

Intuitively, the physical power output from any solar array is dependent on the amount of solar irradiance that the panels are exposed to. Using the PVLib python package from Sandia National Laboratories and "irradiance to DC" and "DC to AC" classes within PVLib created by the National Renewable Energy Lab [27], we were able to convert our Oahu, Hawaii irradiance data into a time series of potential AC power output from all 17 solar arrays. The mathematical formulation behind these python classes is as follows:

$$P_{dc} = G_{poaeff}\frac{P_{dc0}}{1000}(1+\gamma_{pdc}(T_{cell}-T_{ref})) \tag{13}$$

Equation 13 converts an irradiance value (G_{poaeff}) into an equivalent DC wattage given the efficiency of the PV panels ($\frac{P_{dc0}}{1000}$). It also includes the degradation of efficiency (γ_{pdc}) over time that depends on the temperature surrounding the panels, but for our theoretical and strictly computational study, we have ignored all losses of panel efficiency over time as this is not affected in the time resolution of our interest.

$$\eta = \frac{\eta_{norm}}{\eta_{ref}}(-0.0162\zeta - \frac{0.0059}{\zeta} + 0.9858)$$
$$\text{where } \zeta = \frac{P_{dc}}{P_{dc0}} \text{ and } P_{dc0} = \frac{P_{ac0}}{\eta_{norm}} \tag{14}$$

In Equation 14, η denotes the AC power output, and η_{norm} (=0.96) and η_{ref} (=0.9637) represent the nominal and reference inverter efficiencies respectively. Plugging the result from Equation 13 into Equation 14 will output the theoretical AC power timeseries from each of the 17 locations around the Oahu airport.

V. Discussion and Results

The hierarchical control scheme that we have applied to the 17 inverter case study in Figure 6, has been simulated and assessed in its performances meeting a continuous load demand as well as satisfying instantaneous ancillary RegD signal requests. The need for this control system is highlighted in Figure 8, where the uncurtailed output of the solar power plant has no regard for any real-time market

Fig. 6: Satellite image of the distribution of 17 solar irradiance measurement devices around an airport in Oahu, Hawaii. Statistical controller neighboring is indicated by blue, green, and yellow indicators. [26]

requests. Using this uncontrolled system to satisfy real-time and ancillary generation needs would quickly result in malfunctioning hardware, unreliable power, and blackouts on the power grid. Since real-time and ancillary markets require generation to have precise and reliable output, this power plant will require either fossil fuel supporting generation, energy storage, or the proposed smart control capabilities to participate in ancillary markets.

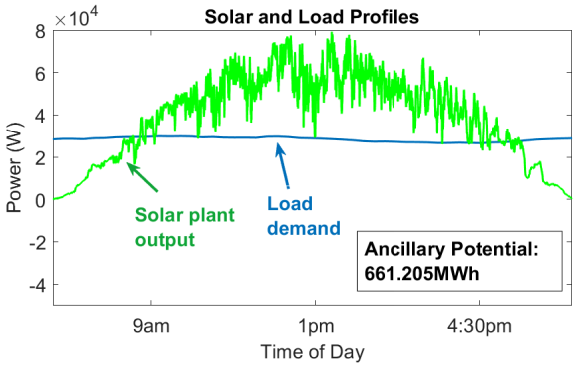

Fig. 8: Solar and load profiles for this case study

In addition to a reduction in fuel-costs and harmful emissions, Figure 8 shows the potential for this 17 inverter solar power plant to satisfy load demand *and* maintain a calculated headroom to satisfy RegD frequency response requests simultaneously. The available headroom of this power plant, after curtailing to a continuous load demand, is shown as the area between the solar plant output (in green) and the load demand (in blue). In this simulation this Ancillary Potential added up to be 661MWh from the day. Any unused ancillary potential from curtailment could either be sent to nearby storage, or dissipated and remain on standby as an operational reserve for ancillary signals like RegD. On today's grid it is common practice for fossil fuelled operational reserves to remain unused until they receive an RegD request, so it is likely that solar power plants will start to participate similarly (not always producing 100% of their potential energy) as we march foreword towards an entirely renewable power system. Without requiring storage to every utility-scale solar power plant, this algorithm will help operators save on storage investment costs.

Utilities in the ancillary service market make money by satisfying RegD signals in real-time. Therefore, their power producing equipment must be fast, responsive, and controlled with precision. In the following results sections we evaluate the performance of our hierarchical control algorithm in contrast to an uncontrolled solar power plant and the newly operational grouping control algorithm in Chile [16].

A. Inverter Signal Communication

Before analyzing the final results of our simulations, we quickly investigate the performance of the signalling and communication within our hierarchical controller for further concept validation. In Figure 7 we witness the output signalling and return signalling of two inverter controllers (on the direct control layer) that have been chosen as virtual neighbors because of their asimilar MPP fluctuations in the hourly statistical analysis from Figure 5.

On both ends of the time interval depicted in Figure 7a we see a reasonably flat maximum power point (MPP) potential from both inveters, which suggests little to no

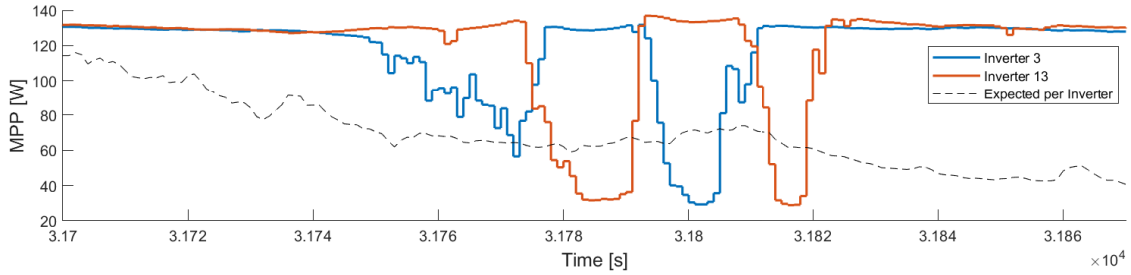

(a) **Output Signal:** Inverter MPP

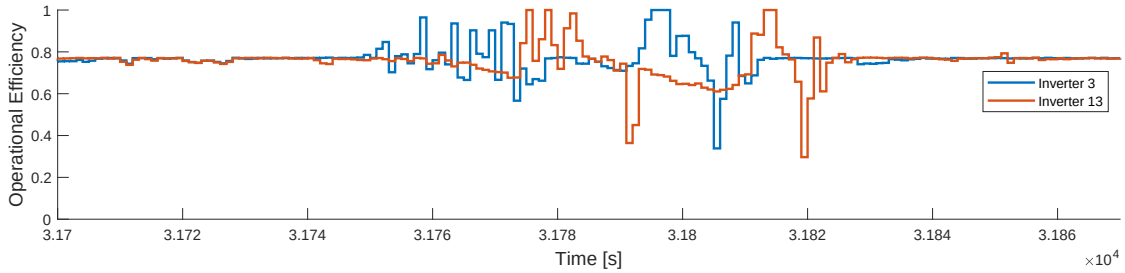

(b) **Return Signal:** Efficiency for Curtailment

Fig. 7: Communication signalling results focused on only two virtually neighboring inverters over a 3 minute window of daily operation.

cloud coverage. However, throughout the middle of the time interval there is a clear cloud-coverage event where the inverters' MPP potentials are being impacted. The MPP status is approximated as explained in equation 5, and is the signal output from the current control layer (in this case the direct control layer) to the above supervisor/central control layer. As the shading crosses the power plant area, the need for help is triggered by the MPP levels falling below the expected power generation ability per inverter (black dashed line), which is the load demand split evenly amongst all 17 inverters.

Figure 7b shows the returned signal –from the supervisor/central layer to the current layer– that communicates the curtailment level the controller should be operating at. At the direct inverter control layer, this can be easily translated into the operational efficiency (equation 10) the controller sets its voltage-current ratio. Although other inverters and groups within this hierarchical controller are influencing the return signal to the two inverters shown in Figure 7b, it is evident that our statistical correlation is being put to use because the efficiencies appear to be peaking at alternating times.

Through the lens of headroom signalling for individual inverters, Figure 10 brings further insight into how the communications between all inverters work together during the cloudy and non-cloudy periods of our simulation. The not cloudy time interval, where sunlight is available to all inverters, Figure 10a shows how all the inverters with positive headroom availability after meeting a load demand curve. Alternatively, Figure 10b expresses the headroom communication signalling when the system is interfacing with cloud coverage. The negative headroom values signify to higher control levels that the inverter is in need of help from other inverters. Throughout this these time domains, the need for requesting help by the second would strongly improve the precision of power output.

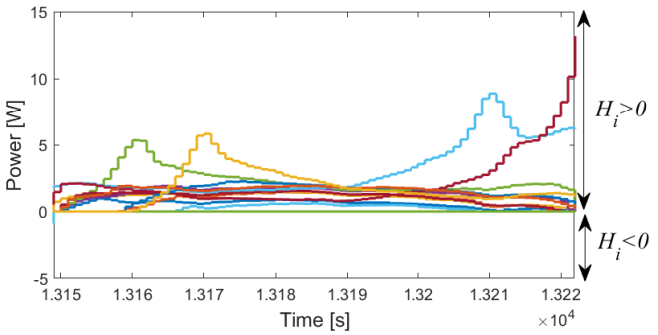

(a) Not Cloudy

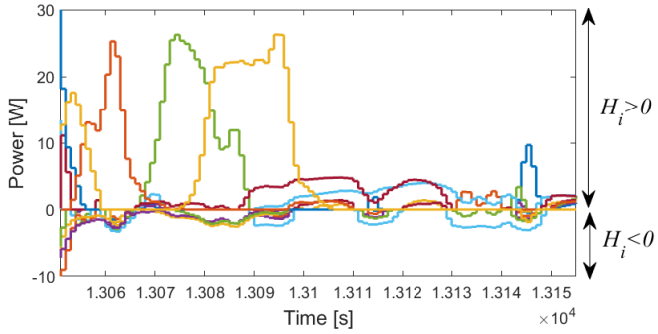

(b) Cloudy

Fig. 10: Communication signalling results focused on only two virtually neighboring inverters over a 3 minute window of daily operation.

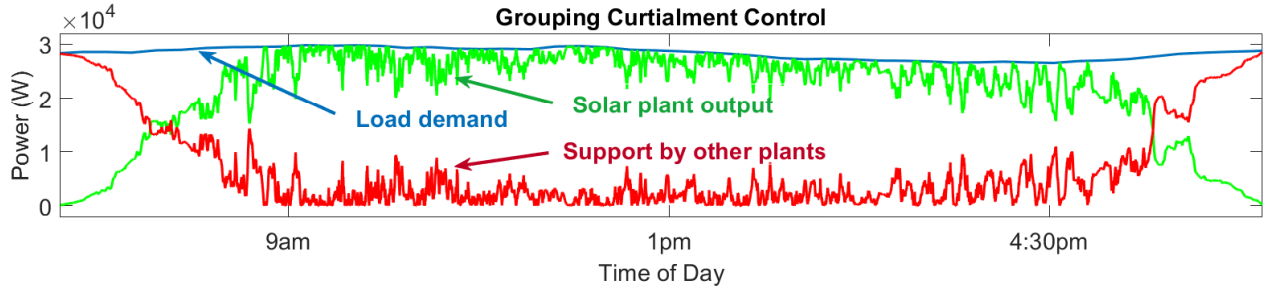

(a) Grouping control (reenacted from [16] to satisfy load demand).

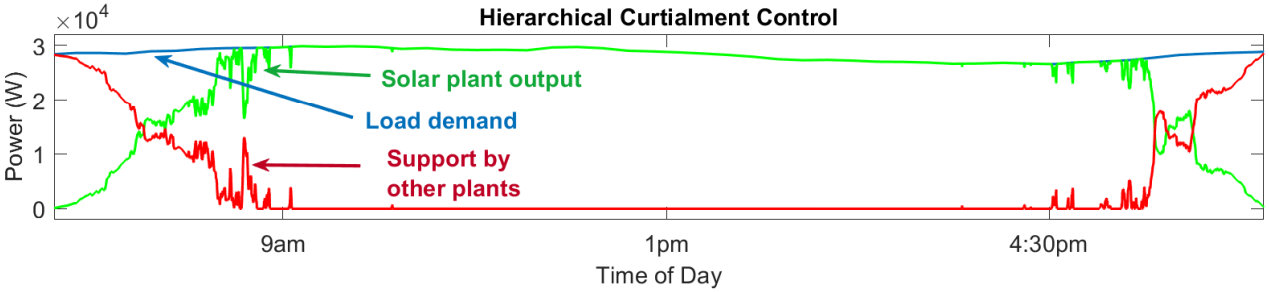

(b) Hierarchical Control

Fig. 9: Hierarchical control example with 6 inverter controllers, 3 supervisor controllers, and one central controller.

With all 17 inverters and 3 supervisor controllers operating under similar signalling and communication, the power output of the system should be able to precisely follow a dynamic load demand curve while managing headroom for ancillary potential.

B. Satisfying a Load Demand

The current solutions for utility operators to manage the unreliability and intermittency of solar power include hybrid power plants –solar arrays that are paired with storage or highly responsive combustion engines– and energy storage. Technologies that have the ability to ramp up and down as fast as cloud coverage changes will be costly, often have far higher carbon footprints, and degrade energy storage systems quickly. Reducing the amount of fluctuations in the red line is what will allow utilities to operate solar power plants without hybrid support systems, which effectively will allow the power grid to depend less on ramp-able fossil fuel technologies like coal and natural gas.

Figure 9 shows the effectiveness of both grouping control and hierarchical control in curtailing a solar power plant to meet a dynamic load demand. Table I quantifies the stability of hierarchical control over grouping control in the simulation.

TABLE I: Summary of Ancillary Service (RegD) Simulations

Control Scheme	**Mileage**	**Regulation**
Grouping Control	2.45 MW	80.89 MWh
Hierarchical Control	0.14 MW	4.35 MWh

Grouping control is effective in many ways (it was even installed onto a real utility-scale plant in Chile), but the algorithmic error does not allow the system to become entirely independent of external power sources to meet its load demand. In Table I, it is clear that hierarchical control has resulted in far less mileage and regulation throughout the simulation. Mileage is a metric used to measure the instantaneous ramping that the solar power plant would require of supportive generation and/or energy storage. Regulation is the total amount of energy that was supplied from generation sources other than the solar power plant in order to maintain the load demand. These metrics confirm to hierarchical control being around 18x more stable than grouping control. Both mileage and regulation are indicators to unstable that enhances the expensive fuel-costs and carbon emissions that utility operators are looking to eliminate.

C. Dispatching by RegD Signal

The ability for a utility-scale solar power plant to participate in the ancillary service market by responding to RegD signalling is the more economically incentivizing side of developing a functional curtailment control algorithm. In February 2021, prices in ERCOT's ancillary service markets jumped from around $8/MWh to $9,000/MWh during a large system blackout. As we aspire to construct net-zero emission power grids in the near future, it will be profitable for both large power grid operators, as well as smaller private generation oweners, to use solar power plants to respond to RegD signals.

As previously mentioned, the simulated power plant could either be used entirely as an operational reserve, or could become multi-purpose by satisfying RegD signals with any unused, curtailed power after meeting a load demand.

TABLE II: Summary of Ancillary Service (RegD) Simulations

Control Scheme	**Plant Response to RegD**
Grouping Control	54.9%
Hierarchical Control	67.4%

Table II summarizes the success-rate of grouping control and hierarchical control in satisfying positive RegD signals (0 to 1) throughout a day. Hierarchical control satisfied about 12% more of the RegD ancillary requests with solar power, and was nearly 100% effective between sunrise and sunset. Grouping control, still showed some evidence of instability by requiring alternative, supporting generation to fulfill nearly half of its RegD requests.

Through direct comparison to the already successful grouping control, installed in a utility-scale Chilean power plant, our simulation results have shown realistic opportunity for hierarchical curtailment control to unlock real-time ancillary services for utilty-scale solar.

VI. Conclusion & Future Directions

The proposed hierarchical curtailment control algorithm is simulating results that appear extremely competitive to participate in both the day-ahead and ancillary energy markets (independently or simultaneously) for utility power plant operators. Being able to participate in these energy markets would mean the utility will be able to undercut the bidding prices of fossil fuel-operators, and eventually monopolize large portions of the market. Eventually, curtailment control technology may be a fundamental component of creating and operating zero-emission, national power systems.

The following are some future directions that would extend from this project.

- Case study application to controlled wind farms.
- Proof of concept with small scale prototype (raspberry pi/ mini panels) in the lab
- Include forecasting methods in hierarchical controller
- Investigate how to expand hierarchical control to a systematic, centralized "smart-grid". (Hierarchical topology would probably not be physically connected but instead *remotely connected* meaning different arrays that are far apart geographically are computationally signalled as neighboring generators. Also harder forecasting implementation.)

- Stability analysis (more mathematical) discerning if centralized/hierarchical control of the entire power system is “better" than traditional decentralized dynamics. (Or at what level would you want to have hierarchical control in action. Centralized per county? Centralized per state? Etc.)

References

[1] O. Ogunrinde, E. Shittu, and K. K. Dhanda. Investing in renewable energy: Reconciling regional policy with renewable energy growth. *IEEE Engineering Management Review*, 46(4):103–111, 2018.

[2] B. Kroposki, B. Johnson, Y. Zhang, V. Gevorgian, P. Denholm, B. Hodge, and B. Hannegan. Achieving a 100% renewable grid: Operating electric power systems with extremely high levels of variable renewable energy. *IEEE Power and Energy Magazine*, 15(2):61–73, 2017.

[3] Aeo2020 electricity. *U.S. Energy Information Administration U.S. Energy Information Admin*, 2020.

[4] National Renewable Energy Lab. Nrel energy models examine the potential for wind and solar grid integration. *NREL Innovation Impact Analysis*, 2013.

[5] Transmission planning and cost allocation by transmission owning and operating public utilities. *UNITED STATES OF AMERICA FEDERAL ENERGY REGULATORY COMMISSION*, Order 1000, 2018.

[6] Electric storage participation in markets operated by regional transmission organizations and independent system operators. *UNITED STATES OF AMERICA FEDERAL ENERGY REGULATORY COMMISSION*, Order 841, 2018.

[7] Thanh Mai, Niyam Haque, Thai Hau Vo, and Phuong Nguyen. Coordinated active and reactive power control for overvoltage mitigation in physical lv microgrids. *Journal of Engineering*, 2019(18):5007–5011, January 2019.

[8] Y. Su, H. Li, Y. Cui, S. You, Y. Ma, J. Wang, and Y. Liu. Adaptive pv frequency control strategy based on real-time inertia estimation. *IEEE Transactions on Smart Grid*, pages 1–1, 2020.

[9] E. I. Batzelis, G. Anagnostou, I. R. Cole, T. R. Betts, and B. C. Pal. A state-space dynamic model for photovoltaic systems with full ancillary services support. *IEEE Transactions on Sustainable Energy*, 10(3):1399–1409, 2019.

[10] Seung-Ho Song, Shin-il Kang, and Nyeon-kun Hahm. Implementation and control of grid connected ac-dc-ac power converter for variable speed wind energy conversion system. In *Eighteenth Annual IEEE Applied Power Electronics Conference and Exposition, 2003. APEC '03.*, volume 1, pages 154–158 vol.1, 2003.

[11] F. Baccino, F. Conte, S. Grillo, S. Massucco, and F. Silvestro. An optimal model-based control technique to improve wind farm participation to frequency regulation. *IEEE Transactions on Sustainable Energy*, 6(3):993–1003, 2015.

[12] M. El Mokadem, V. Courtecuisse, C. Saudemont, B. Robyns, and J. Deuse. Experimental study of variable speed wind generator contribution to primary frequency control. *Renewable Energy*, 34(3):833 – 844, 2009.

[13] Jesper Runge Kristoffersen and Peter Christiansen. Horns rev offshore windfarm: Its main controller and remote control system. *Wind Engineering*, 27:351–359, 09 2003.

[14] H. Karbouj and Z. H. Rather. Voltage control ancillary service from wind power plant. *IEEE Transactions on Sustainable Energy*, 10(2):759–767, 2019.

[15] J. Tan and Y. Zhang. Coordinated control strategy of a battery energy storage system to support a wind power plant providing multi-timescale frequency ancillary services. *IEEE Transactions on Sustainable Energy*, 8(3):1140–1153, 2017.

[16] Vahan Gevorgian. Highly accurate method for real-time active power reserve estimation for utility-scale photovoltaic power plants.

[17] Vahan Gevorgian and Barbara O'Neill. Advanced grid-friendly controls demonstration project for utility-scale pv power plants.

[18] X. Chen, Y. Du, H. Wen, L. Jiang, and W. Xiao. Forecasting-based power ramp-rate control strategies for utility-scale pv systems. *IEEE Transactions on Industrial Electronics*, 66(3):1862–1871, 2019.

[19] James R. Nelson and Nathan G. Johnson. Model predictive control of microgrids for real-time ancillary service market participation. *Applied Energy*, 269:114963, 2020.

[20] Anuj Banshwar, Naveen Kumar Sharma, Yog Raj Sood, and Rajnish Shrivastava. Renewable energy sources as a new participant in ancillary service markets. *Energy Strategy Reviews*, 18:106 – 120, 2017.

[21] H.H. Zeineldin, Kankar Bhattacharya, Ehab El-Saadany, and M.M.A. Salama. Impact of intentional islanding of distributed generation on electricity market prices. *Generation, Transmission and Distribution, IEE Proceedings-*, 153:147 – 154, 04 2006.

[22] Debra Lew, Lori Bird, Michael Milligan, Bethany Speer, Xi Wang, Enrico Maria Carlini, Ana Estanqueiro, Damian Flynn, Emilio Gomez-Lazaro, Nickie Menemenlis, et al. *Wind and solar curtailment*. National Renewable Energy Laboratory, 2013.

[23] S. Davis. Solar system efficiency: Maximum power point tracking is key. *Power Electronics Technology*, 2015.

[24] Mihnea Rosu-Hamzescu and Sergiu Oprea. Practical guide to implementing solar panel mppt algorithms. *Microchip Technology Inc, Application Note, AN1521*, 2013.

[25] H. Patel and V. Agarwal. Maximum power point tracking scheme for pv systems operating under partially shaded conditions. *IEEE Transactions on Industrial Electronics*, 55(4):1689–1698, 2008.

[26] M. Sengupta and A. Andreas. Oahu solar measurement grid (1-year archive): 1-second solar irradiance; oahu, hawaii (data). *NREL Report No. DA-5500-56506.*, 2010.

[27] William F. Holmgren, Clifford W. Hansen, and Mark A. Mikofski. pvlib python: a python package for modeling solar energy system. *Journal of Open Source Software*, 2018.